

Mechanisms of Discrimination between Cobalamins and Their Natural Analogues during Their Binding to the Specific B₁₂-Transporting Proteins[†]

Sergey N. Fedosov,^{*,‡} Natalya U. Fedosova,[§] Bernhard Kräutler,^{||} Ebba Nexø,[⊥] and Torben E. Petersen[‡]

Protein Chemistry Laboratory, Department of Molecular Biology, University of Aarhus, Science Park, Gustav Wieds Vej 10, DK 8000 Aarhus C, Denmark, Institute of Physiology and Biophysics, Department of Biophysics, University of Aarhus, Ole Worms Alle 1185, DK 8000 Aarhus C, Denmark, Institute of Organic Chemistry and Center of Molecular Biosciences, University of Innsbruck, Innrain 52A, Innsbruck A-6020, Austria, and Department of Clinical Biochemistry, AS Aarhus University Hospital, Nørrebrogade 44, DK 8000 Aarhus C, Denmark

Received October 4, 2006; Revised Manuscript Received February 9, 2007

ABSTRACT: Three proteins, intrinsic factor (IF), transcobalamin (TC), and haptocorrin (HC), all have an extremely high affinity for the cobalamins (CbIs, $K_d \approx 5$ fM) but discriminate these physiological ligands from Cbl analogues with different efficiencies decreasing in the following order: IF > TC > HC. We investigated interactions of these proteins with a number of ligands: Cbl, fluorescent conjugate CBC, two base-off analogues [pseudo-coenzyme B₁₂ (pB) and adenosyl factor A (fA)], and a baseless corrinoid cobinamide. Protein–ligand encounter and the following internal rearrangements in both molecules were registered as a change in the fluorescence of CBC (alone or mixed with other ligands), a transition in absorbance of pB and fA (base-off → on-base conversion), and alterations in the molecular mass of two split IF domains. The greater complexity of the binding kinetics followed better Cbl specificity (HC < TC < IF). On the basis of the experimental results, we propose a general binding model with three major steps: (1) initial attachment of the ligand to the high-affinity C-domain, (2) primary assembly of N- and C-domains, and (3) slow adjustments and fixation of the ligand at the domain–domain interface. Since step 3 was characteristic of highly specific TC and especially IF, we suggest its particular importance for ligand recognition. The designed models revealed the absolute K_d values for a group of analogues. Calculations show that most of them could potentially bind to the specific transporters IF and TC under physiological conditions. Implications of this finding and the protective role of HC are discussed.

Cobalamin (Cbl,¹ vitamin B₁₂) is an important cofactor in human metabolism (*1*). It is produced only by bacteria, while animals (humans included) obtain vitamin B₁₂ via an intricate food chain. Microorganisms also synthesize various Cbl-resembling molecules, the analogues, which have no catalytic activity in human cells. The selective uptake of Cbl by humans requires three transporting proteins: intrinsic factor (IF), transcobalamin (TC), and haptocorrin (HC) (see reviews *1–3*). IF is responsible for intestinal uptake of vitamin B₁₂. TC is the major plasma transporter. HC seems to be a scavenging protein. All binders have very high affinities for Cbl, though controversy on this subject still exists with exceptional dispersion in the reported values [$K_d = 10^{-15}$ – 10^{-9} M (*4–11*)]. In our previous publications, we have

analyzed the background of possible errors leading to underestimated affinity. Among typical cases are (i) nonoptimal refolding of the purified protein (discussed in ref *10*), (ii) denaturation of the protein during prolonged incubation (observed in ref *11*), (iii) insufficient equilibration time for the protein/ligand mixture, and (iv) incorrect fitting models (iii and iv discussed in ref *9*). With all premises taken into account, the lowest dissociation constants of 10^{-15} M can be measured for all Cbl binding proteins (*6, 7, 9, 10*).

Besides exceptional affinity for Cbl, two carriers of major importance (IF and TC) are characterized by high specificity for the true substrate Cbl (*2, 4, 12*). On the other hand, the third protein (HC) binds a variety of corrinoids with approximately equal strength (*2, 4, 12*). Unfortunately, most of the available binding data are hardly applicable for accurate calculations. First, the relative affinities $K_{\text{analogue}}/K_{\text{Cbl}}$ are the only parameters presented for most corrinoids. Second, incubation of the binding mixture (analogue, Cbl, and the binding protein) is typically too short to reach complete equilibration, as discussed in ref *11*. Finally, high dispersion in the reported K_{Cbl} values is a serious obstacle to evaluation of the K_{analogue} values expressed in concentration units. A detailed knowledge of interactions between Cbl analogues and the Cbl-specific proteins is, however, critical for (i) accurate measurement of corrinoids in biological samples, (ii) prediction of the distribution of Cbl and

[†] This work was supported by the Lundbeck foundation Cobento A/S.

* To whom correspondence should be addressed. Telephone: (+45) 89 42 50 92. Fax: (+45) 86 13 65 97. E-mail: snf@mb.au.dk.

[‡] Department of Molecular Biology, University of Aarhus.

[§] Department of Biophysics, University of Aarhus.

^{||} University of Innsbruck.

[⊥] AS Aarhus University Hospital.

¹ Abbreviations: AdoCbl, 5'-deoxy-5'-adenosylcobalamin (adenosylcobalamin, coenzyme B₁₂); Cbi, dicyanocobinamide; Cbl, cobalamin (upper group not specified); CBC, fluorescent conjugate of CNCbl; CNCbl, cyanocobalamin (vitamin B₁₂); fA, adenosyl-factor A (adenosyl-2'-methyladeninylcobamide); HC, haptocorrin; IF, intrinsic factor; pB, pseudo-coenzyme B₁₂ (adenosyladeninylcobamide); P_i buffer, NaH₂PO₄/Na₂HPO₄ buffer; TC, transcobalamin.

analogue between transporting proteins and cell compartments, and (iii) correct application of Cbl-based conjugates with imaging and therapeutic properties (10, 13, 14).

Up to now, very few hypotheses explaining the mechanism of Cbl recognition have been proposed (5, 9, 12). This is regrettable, since the described combination of exceptional binding strength and a widely varying specificity presents an example of protein–ligand interactions of general interest. The availability of recombinant TC (15, 16) and IF (7, 17) stimulated investigation of Cbl binders via different approaches. Eventually, a plausible scheme of interaction between IF and Cbl was put forward. Thus, a two-domain organization was suggested for IF, whose two separate domains, when cleaved into the N-terminal peptide IF₃₀ and the C-terminal glycopeptide IF₂₀, were efficiently reassembled by Cbl (18). The two-domain architecture was established for the kindred protein TC by crystallographic analysis (19). In the obtained structure of TC·Cbl, the attached ligand was sandwiched between N- and C-terminal parts of the protein corresponding to the analogous domains of IF. The two binding units seem to have different functions. Thus, efficient binding of Cbl to the isolated C-terminal fragment (IF₂₀) was observed, whereas a very weak binding to the N-terminal unit (IF₃₀) was found under similar conditions (9, 10, 18). This suggests the C-terminal segment as a primary binding site, yet formation of the binding site is completed only after assembly of N- and C-terminal units (9, 10, 18). The ligand-promoted domain–domain contacts may be important for discrimination between Cbl and other corrinoids. Additionally, association of two binding units was critical for the receptor recognition of the Cbl-saturated IF (9).

We report here a comparative study of the interactions between several corrinoids of different geometry and three transporting proteins (IF, TC, and HC). Quantification of the binding–dissociation kinetics is carried out by fluorescent and absorbance methods, and dissociation constants for several Cbl analogues are calculated in the absolute concentration units. Application of ligands with deviating structures decelerates conformational changes in the protein–ligand complexes and reveals a number of clearly distinguishable transitions. The critical steps of substrate recognition are established, where the correct adjustment of assembled domains seems to be the prerequisite for specific binding. Physiological and medical implications are discussed.

EXPERIMENTAL PROCEDURES

Materials

All standard chemicals were purchased from Merck and Sigma-Aldrich. AdoCbl and the baseless analogue dicyano-Cbi were obtained from Sigma-Aldrich. The fluorescent conjugate CBC was kindly provided by Ch. Grissom (10). Adenosyl-pseudo-B₁₂ (pseudo-coenzyme B₁₂, pB) and adenosyl factor A (fA), two natural base-off analogues of AdoCbl, were synthesized as described elsewhere (20).

Methods

Preparation of Cbl Binding Proteins. Recombinant human TC and IF were produced from yeast and plants, respectively,

as described in our previous publications (15–18). HC was purified from human plasma (21). All proteins were initially obtained as Cbl-saturated holo forms. The unsaturated apo forms of HC and TC were prepared by denaturing in 5–8 M guanidine hydrochloride (7), while IF was treated with 8 M urea (10). Renaturing was conducted by dialysis in 0.2 M P_i buffer (HC and TC) or fast dilution (IF) (see refs 7 and 10 for details).

Measurement of the Binding–Dissociation Kinetics with Fluorescent Probe CBC. Binding of the fluorescent Cbl derivative CBC to a Cbl-specific protein is accompanied by an increase in the quantum yield of its fluorescence (10). Dissociation causes an opposite effect. Competition between CBC and a nonfluorescent ligand X (e.g., AdoCbl, pB, fA, or Cbi) changes the time dependence of binding in accordance with the relevant rate constants. In such a way, CBC was used as a tool to analyze interaction of several corrinoids (0.55 μM) with HC, TC, and IF (0.5 μM). Details of the approach are explained in our previous publication (10). The measurements were performed on a DX.17MV stopped-flow spectrofluorometer (Applied Photophysics), using an excitation wavelength of 525 nm (bandpass of 7 nm) with a 550 nm cutoff filter on the emission side. The reaction medium was 0.2 M P_i buffer at pH 7.5 and 20 °C. During the long-time dissociation experiments, the emission spectra of (1) a protein/X/CBC mixture, (2) a protein/CBC mixture, and (3) CBC were measured at each time point and used in calculations as explained elsewhere (10).

Absorbance Measurements. Interaction of a ligand (20 or 40 μM) with a binding protein (20 μM) was followed in 0.2 M P_i buffer at pH 7.5 and 20 °C by changes in absorbance at indicated wavelengths (see the text and figures). Kinetics of the spectral transition was recorded on a DX.17MV stopped-flow spectrofluorometer from Applied Photophysics (bandpass of 18.6 nm, light path of 1 cm). The dead time of the stopped-flow mixing was determined to be 1.6 ± 0.2 ms.

Determination of the Molecular Mass by Laser Light Scattering. Molecular masses of the associating IF fragments were determined by analysis of static light scattering as described previously (18). In short, the protein preparation (100 μL, 100–300 μg) with or without added ligand was applied to a Superose-12 HR 30 column equilibrated with 0.1 M Tris and 0.2 M NaCl (pH 7.5). Gel filtration was performed on a HPLC system LC-10Advp (Shimadzu Corp.), where the light scattering, refractive index, and absorbance were measured by in-line detectors MiniDAWN (Wyatt Technology Corp.), RID-10A (Shimadzu Corp.), and SPD-10Av (Shimadzu Corp.). Calculation of the molecular masses of the proteins was based on proportionality between the light scattering and the product of the weight-average molar mass and the concentration of the macromolecule (milligrams per milliliter).

Data Fitting. Simple kinetic reactions were fitted using program KyPlot 4 (Kyence Inc.) and the appropriate equations (9). Complex reactions were simulated and fitted using Gepasi 3.2 (22) supplied by kinetic schemes presented in the text.

RESULTS

We tested several types of ligands, where substitutions or deletions were introduced into the core structure of Cbl.

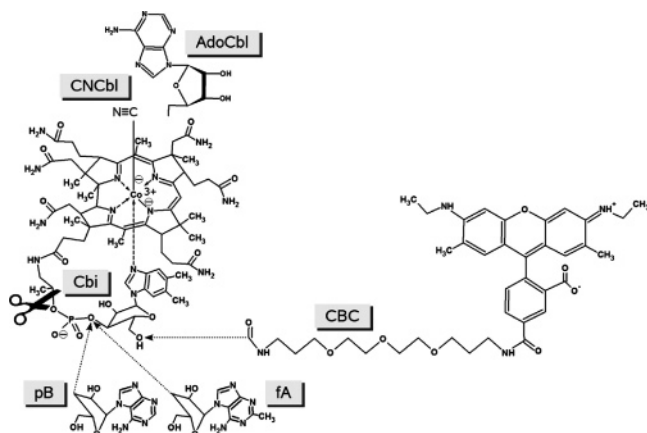


FIGURE 1: Structures of the corrinoids employed in this study. Detailed information can be found in refs 1, 10, and 20.

Sketchy drawings (Figure 1) are given for (1) the “true” coenzyme AdoCbl, (2) fluorescent conjugate CBC, (3) two “base-off” analogues pB and fA with substituted nucleotides, and (4) the incomplete corrinoid Cbi lacking the whole nucleotide moiety. Detailed structures of the ligands given above can be found elsewhere (1, 10, 20). The tracing analogue CBC (Figure 1) contained the fluorescent rhodamine group connected via a spacer to the 5'-OH-ribosyl group of CNCbl (10). Interactions of CBC with two specific proteins, IF and TC, were characterized in our previous publication (10). Its binding was quite efficient and accompanied by a significant increase in the magnitude of the fluorescent signal upon formation of the protein–CBC complexes. This makes CBC a convenient tool for monitoring the binding kinetics of other nonfluorescent corrinoids (or X-ligands, as they are presented in the schemes).

The described corrinoids interacted with three specific transporting proteins: human haptocorrin (HC), recombinant human transcobalamin (TC), and recombinant human intrinsic factor (IF). Various binding–dissociation experiments were conducted on different time scales to reveal the details of binding kinetics.

Determination of Relative Affinities. To simplify comparison between earlier and current data, we have conducted a binding assay according to a typical isotope dilution method (12). The following ratios of the apparent dissociation constants were obtained for HC ($K_{\text{analogue}}/K_{\text{Cbl}} \approx 1$, all ligands in the study), TC ($K_{\text{pB}}/K_{\text{Cbl}} = K_{\text{fA}}/K_{\text{Cbl}} = 5$, $K_{\text{Cbi}}/K_{\text{Cbl}} = 2000$), and IF ($K_{\text{pB}}/K_{\text{Cbl}} = 200$, $K_{\text{fA}}/K_{\text{Cbl}} = 300$, $K_{\text{Cbi}}/K_{\text{Cbl}} = 10^5$). The two reference ligands (CNCbl and AdoCbl) did not differ from each other and are notated as Cbl. It should be explicitly stated that the true equilibrium was hardly reached under the conditions of the experiment (50 pM binding protein, 50 pM radioactive CNCbl, and 10 pM to 600 nM nonradioactive ligand for 20 h at 4 °C). Therefore, the presented relative affinities are called apparent.

Transient Kinetic Experiments on the 0–0.2 s Time Scale. The individual protein (HC, TC, or IF) was rapidly injected into either CBC alone or a mixture of ligands CBC and X, where X stands for one of the nonfluorescent compounds, AdoCbl, fA, pB, or Cbi (Figure 2). Formation of the protein–CBC complex was monitored over time due to an increase in the fluorescence of CBC upon its attachment to the specific binder (10). The presence of a nonfluorescent ligand X together with CBC has made ramifications in the reaction

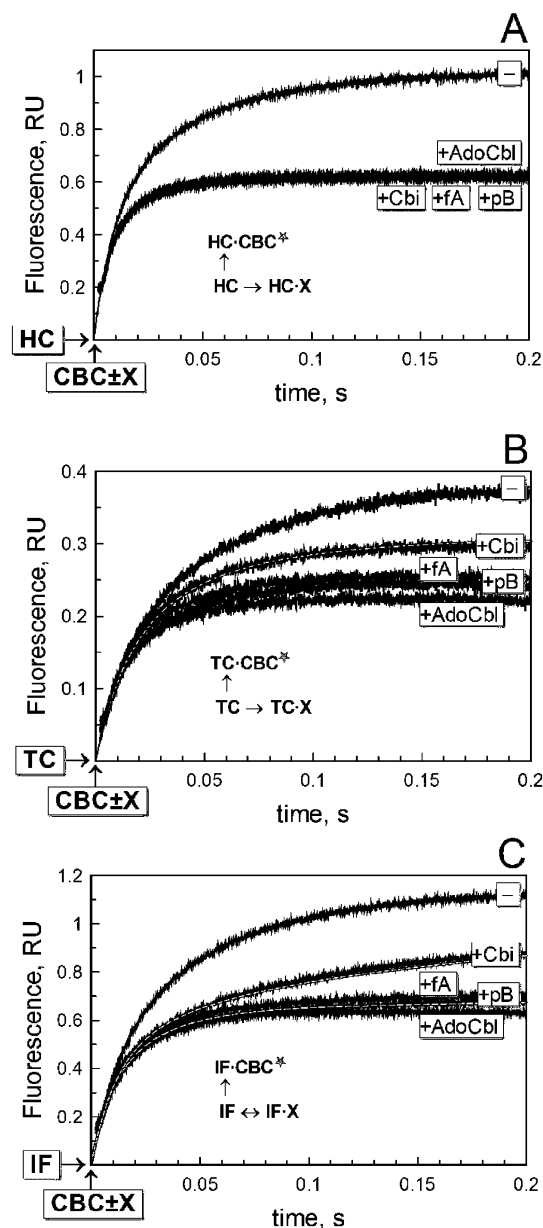


FIGURE 2: Fluorescent binding kinetics on the 0–0.2 s time scale. Binding proteins (0.5 μM) were added to the mixtures of ligands 0.55 μM CBC and 0.55 μM X (X represents none, AdoCbl, pB, fA, or Cbi) at pH 7.5 and 20 °C. Dashed lines show simulations according to the general fitting models (see the text). Binding experiments are performed with HC (A), TC (B), and IF (C).

route, resulting in formation of both the fluorescent protein–CBC complex and an invisible protein–X complex. Since two ligands compete for the same protein, the transient and final levels of fluorescence would depend on the attachment rate constants and relative stabilities of both complexes.

The kinetic behavior of HC and TC on a short time scale (Figure 2A,B) could be approximated by an irreversible binding mechanism, where the final level of fluorescence depended on the ratio between the attachment rate constants $k_{+\text{CBC}}$ and $k_{+\text{X}}$. They were calculated by computer simulations as described previously (10). The obtained values are presented in Table 1.

The third protein (IF) demonstrated deviation from a simple irreversible binding when the analogues Cbi, pB, and fA were supplemented as ligand X (Figure 2C). Thus,

Table 1: Binding Rate Constants for Different Corrinoids at 20 °C and pH 7.5

	k_{+1} (M ⁻¹ s ⁻¹)			k_{-1app} (s ⁻¹), ^b IF (reverse)
	HC	TC	IF	
CNCbl ^a	≈90 × 10 ⁶	68 × 10 ⁶	74 × 10 ⁶	≈0
AdoCbl	78 × 10 ⁶	52 × 10 ⁶	65 × 10 ⁶	≈0
CBC	124 × 10 ⁶	68 × 10 ⁶	77 × 10 ⁶	≈0
pB	77 × 10 ⁶	40 × 10 ⁶	70 × 10 ⁶	1.6
fA	76 × 10 ⁶	33 × 10 ⁶	56 × 10 ⁶	0.8
Cbi	73 × 10 ⁶	17 × 10 ⁶	57 × 10 ⁶	10

^a Data from refs 10 and 16. ^b The apparent dissociation rate constants were calculated for the experiments, where partial dissociation of the IF·X complex could not be ignored.

additional formation of the IF·CBC complex was visible on the time scale of 0.05–0.2 s as a consequence of partial dissociation of the IF·X complex. These experiments were fitted to the reversible mechanism with the parameter k_{-X} added. The calculated values of k_{-X} are listed in Table 1, yet these coefficients are apparent and influenced by the following binding steps.

Binding and Dissociation Kinetics on the 0.1–200 s Time Scale. A set of experiments, analogous to those in the previous section, was conducted on a longer time scale (Figure 3). This was expected to reveal additional steps in the competitive binding process. As discussed above, lower levels of fluorescence reflected favorable formation of invisible protein–X complexes. Invariable and weak signals in HC and AdoCbl-, Cbi-, pB-, and fA-containing mixtures (Figure 3A) proved strong retention of all X ligands by HC. The same was valid for the TC with bound AdoCbl and base-off analogues pB and fA (Figure 3B). On the other hand, the baseless corrinoid Cbi with a low affinity for TC (4, 7, 12) behaved differently in the CBC + TC + Cbi reaction (Figure 7B). The ligands were initially bound to TC in a ≈0.3 TC·Cbi/TC·CBC ratio (time interval of 0–0.2 s), but then Cbi completely dissociated from TC, since fluorescence increased up to the maximal level (Figure 3B). The reaction seemed to be driven at different time by the following fluxes: (i) attachment of both ligands TC·CBC ← TC → TC₁·Cbi (0–0.2 s), (ii) first redistribution of ligands TC·CBC ← TC ← TC₁·Cbi → TC₂·Cbi (0.2–5 s), and (iii) final redistribution of ligands TC·CBC ← TC ← TC₁·Cbi ← TC₂·Cbi (5–20 s). Each of the above schemes is characterized by a particular combination of rate coefficients, which can be extracted by sequential analysis of the curve along the time scale (see below). The most specific protein IF bound and exchanged the analogues for CBC in a similar manner within 20 s for Cbi and 200 s for pB or fA (Figure 3C). Formation and dissociation of IF–analogue and TC–Cbi complexes was approximated by a two-step binding mechanism (schemes in Figure 3B,C). To improve fitting, the experiments on Cbi versus CBC competition were also performed on a shorter time scale (0–20 s in the case of TC and 0–5 s in the case of IF) (not shown). The estimated rate constants were afterward adjusted to the general models presented below.

Dissociation Kinetics on 0.1–200 s and 100 h Time Scales. In the following experiments, we have changed the order of mixing. Thus, a protein was allowed to equilibrate for 10 or 60 min with a nonfluorescent ligand X prior to injection of

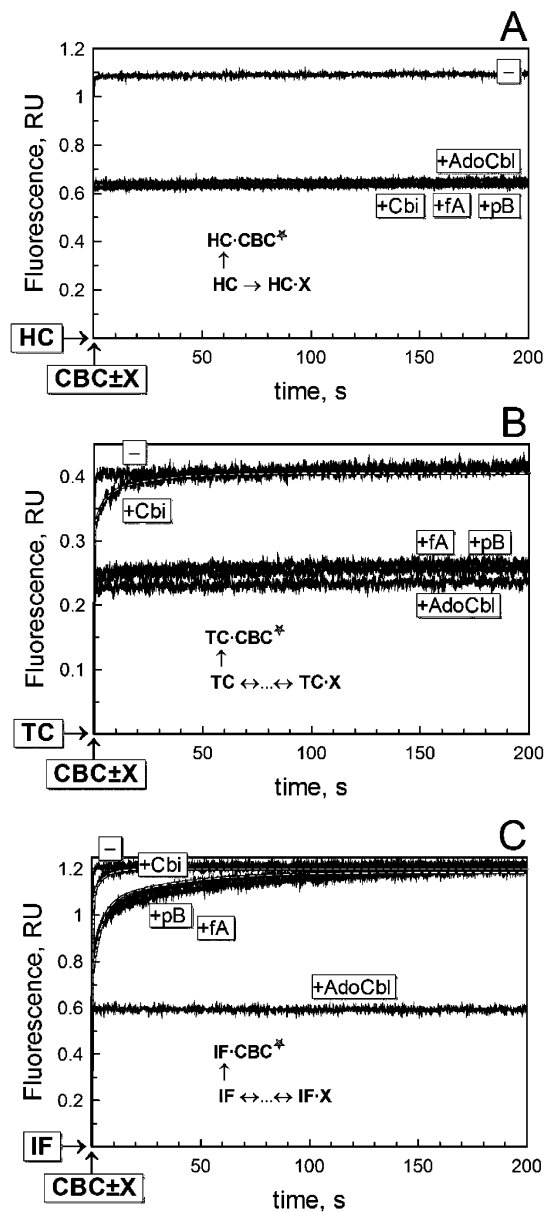


FIGURE 3: Fluorescent binding and dissociation kinetics on the 0.1–200 s time scale. Binding–dissociation experiments were performed with HC (A), TC (B), and IF (C). Experimental conditions as in Figure 2.

CBC. Then, displacement of X by CBC was followed by the increase in fluorescence (Figure 4). The time of 10 min was apparently sufficient for complete equilibration, because additional incubation for up to 60 min had no effect on the dissociation patterns (not shown).

Injection of CBC into any of the saturated HC·X complexes did not induce a change in signal (Figure 4A, bottom curves). In other words, no visible dissociation of the HC·X complex was observed during the first 200 s.

The same result was obtained for TC pre-equilibrated with AdoCbl or two base-off analogues pB and fA (Figure 4B, bottom curves). However, a slow transition was recorded for the TC·Cbi/CBC mixture (Figure 4B, central curve). Mind the difference between two apparently similar dissociating experiments in Figures 3B and 4B. In the first case, no preliminary equilibration of TC with Cbi was carried out, and a rapidly formed TC·Cbi complex dissociated in 30 s (Figure 3B). In the second case, the TC·Cbi complex was

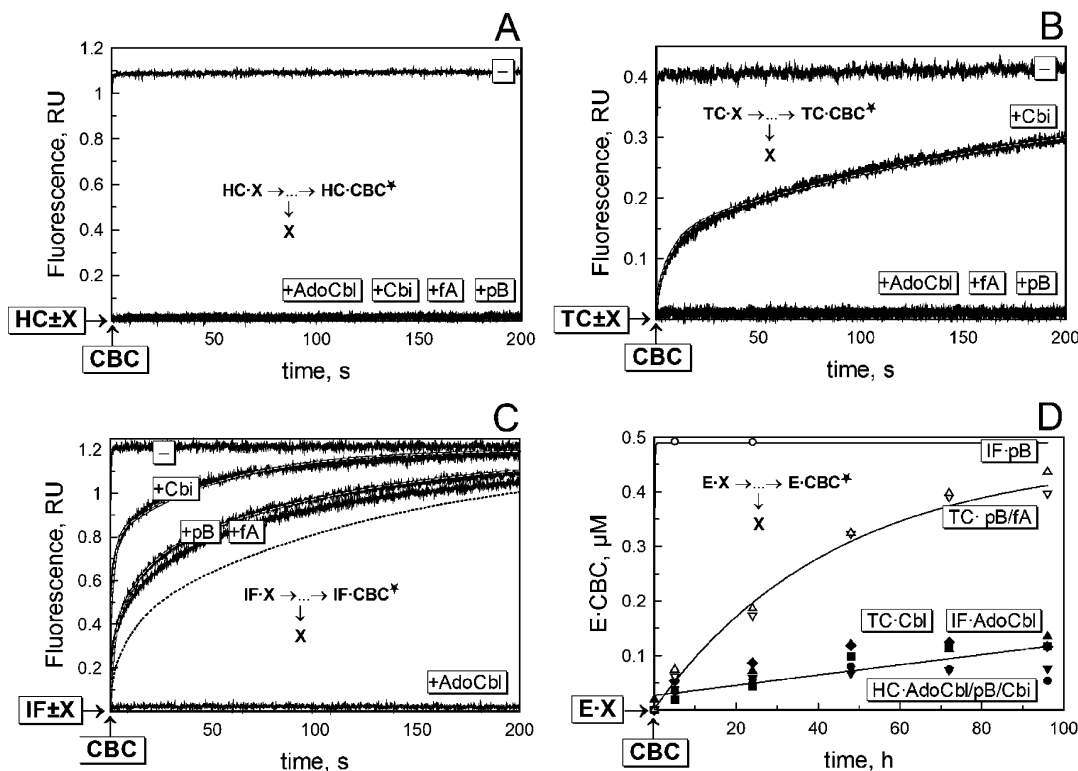


FIGURE 4: Fluorescence dissociation kinetics on 0–200 s and 100 h time scales. Binding proteins (0.5 μM), saturated with a nonfluorescent ligand X (none, AdoCbl, pB, fA, or Cbi, each at 0.55 μM), were mixed with CBC (0.55 μM). The initial 200 s of dissociation of X from HC (A), TC (B), and IF (C) is presented. Panel D summarizes the dissociation process for all proteins over the 100 h time course.

preincubated for 10 min which resulted in a much slower dissociation (Figure 4B). This difference suggests slow tightening of the bonds between TC and Cbi.

A similar fixation of analogues was also discovered for IF when this protein was preincubated with Cbi, pB, or fA prior to CBC binding. The data in Figure 4C demonstrate that the pre-equilibrated IF·X samples (Figure 4C) dissociated much slower than their counterparts in the experiments with simultaneous injection (Figure 3C).

Figure 4D presents a long-term experiment, when dissociation of different complexes was initiated by added CBC and followed over a considerable period of time (100 h). All recorded curves fell into three groups according to the velocity of the registered changes: (1) fast dissociation of all IF–analogue complexes (e.g., IF·pB, top curve in Figure 4D), (2) gradual dissociation of the base-off ligands pB and fA from TC (central curve in Figure 4D), and (3) slow dissociation of IF·AdoCbl and TC·AdoCbl complexes, as well as all HC·X complexes (bottom curves in Figure 4D). The low-velocity group was treated as one set of points because of their significant overlapping and dispersion of points.

The apparent values of the dissociation rate constants from all experiments are listed in Table 2. In many cases, dissociation was not exponential and required multiexponential fits, e.g., IF·Cbi, IF·pB, and TC·Cbi. The calculated phases are given in the percentage of the total amplitude, and they are supplemented with the matching rate coefficients (Table 2). The complex character of dissociation indicates the presence of multiple equilibria inside the protein–ligand pool, where sequential or simultaneous detachment from different complexes (e.g., IF₁·Cbi, IF₂·Cbi, and IF₃·Cbi) may

take place. A more detailed kinetic analysis is presented below.

Spectral Analysis of the Base-Off ↔ Base-On Transition upon Binding to Proteins. Changes in the base-on–base-off configuration of the corrinoids can be monitored with the help of absorbance spectrophotometry (20). We used this feature to test ligands upon their binding to the specific proteins. The predominantly base-off analogues pB and fA are especially useful, because the transition between on- and off-forms involves a change in the cobalt coordination and is accompanied by noticeable shifts in their absorbance spectra. The records in Figure 5 present spectra of three Ado corrinoids (Cbi, pB, and fA) bound either to the specific proteins HC, TC, and IF (A, B, and C, respectively) or in the solution (D). Spectra of AdoCbl in buffers at pH 7.5 and 2 represent exclusively base-on (b-on) and base-off (b-off) conformations, respectively. The corresponding notation is shown in Figure 1.

Binding of analogues pB and fA was accompanied by a shift in their internal base-off ↔ base-on coordination equilibria toward the base-on form (arrows in Figure 5A–C). This effect was particularly expressed in TC·pB and TC·fA complexes (Figure 5B), whereas the binding to HC or IF was characterized by a lower degree of conversion (Figure 5A,C). Be mindful that >99% of all ligands were bound to the protein under the experimental conditions. Therefore, incomplete spectral shifts may point to incomplete conversion with one intermediate form bound (e.g., IF·pB_x) or/and the existence of multiple protein–ligand complexes (e.g., IF₁·pB_{off} ↔ IF₂·pB_{on}).

When pB was mixed with either the N-terminal IF-fragment (IF₃₀) or the C-terminal glycopeptide (IF₂₀), no

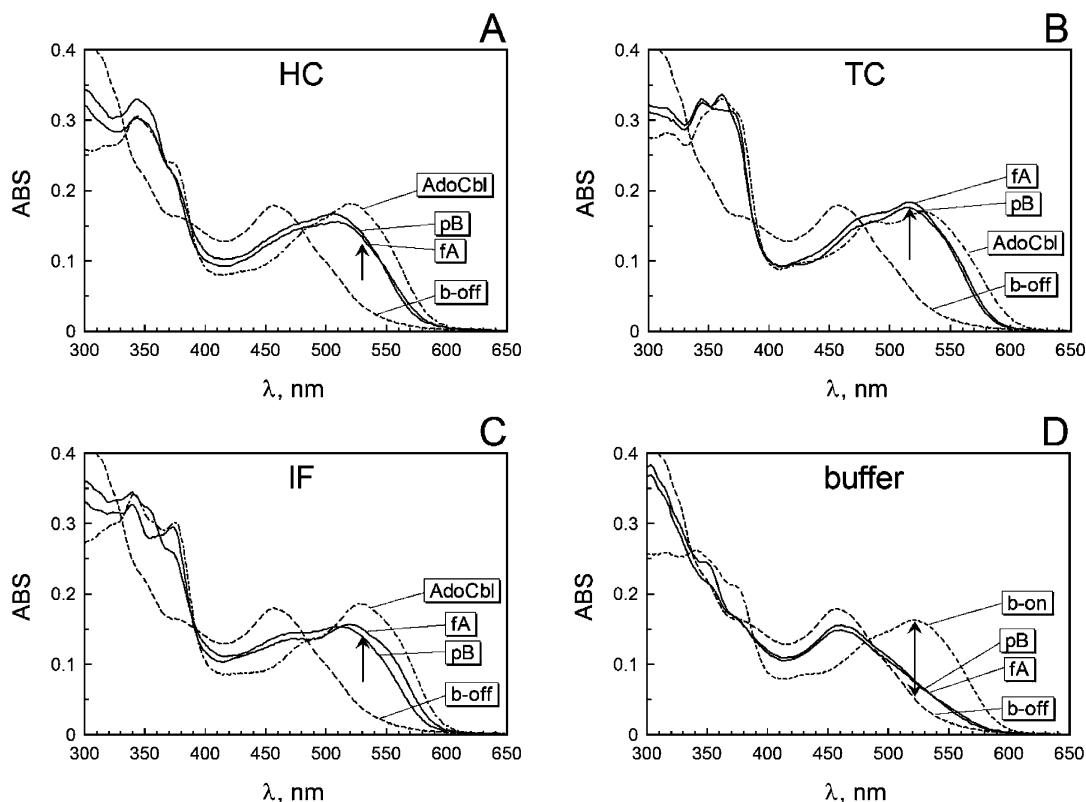


FIGURE 5: Absorbance spectra of ligands upon the base-off \leftrightarrow base-on transition. Ligands AdoCbl, pB, and fA ($20 \mu\text{M}$) were mixed with the binding proteins ($25 \mu\text{M}$) at pH 7.5 and 20°C . Spectra of apoproteins have been subtracted. Dashed lines “b-off” and “b-on” indicate the control spectra of AdoCbl at pH 2 and 7.5, respectively. Arrows indicate the direction of the shift. Spectral characteristics of the ligands in the presence of HC (A), TC (B), and IF (C) and in the buffer (D).

essential change in its spectrum was recorded (not shown). In the first case, no actual binding of pB to IF₃₀ took place. In the second case, pB did bind to IF₂₀ with the expected saturation level of $>90\%$ at $20 \mu\text{M}$ (see Association of IF Fragments in the Presence of Cbl and Analogues), yet the attachment did not cause any significant perturbation in the spectrum of the analogue.

Kinetics of the Base-Off \rightarrow Base-On Transition. Model experiments on coordination of Bzm to AdoCbl in the solution demonstrated a very fast conversion between the on- and off-forms upon pH jumps from 2 to 7.5 ($k > 1000 \text{ s}^{-1}$). Thus, the two coordination forms behave as rapidly equilibrating species and can be treated as a one pool of molecules, where the intramolecular equilibrium is shifted in one direction or another. This assumption essentially simplifies the kinetic interpretation of the binding process. In the experiments described below, Ado ligands, AdoCbl, pB, or fA (20 or $40 \mu\text{M}$), were rapidly mixed with one of the specific proteins ($20 \mu\text{M}$), and an increase in absorbance was recorded.

The absorbance of the base-on ligand AdoCbl changed instantaneously upon its addition to HC (Figure 6A), and this jump seems to be concurrent with attachment of the substrate to the protein. A similar pattern was found for two other proteins, where an additional (conformational?) phase (5–20% of the total amplitude) developed rapidly ($k > 100 \text{ s}^{-1}$) upon interaction of AdoCbl with TC (Figure 6B) and IF (Figure 6C).

Changes in the absorbance of pB and fA (Figure 6) in the visible range of their spectra (arrows in Figure 5) were chosen to follow the process of base coordination to Co^{3+}

ion. All proteins demonstrated an explicit transition following initial attachment of the base-off analogues. The kinetics of this transition was independent of the initial ligand concentration, 20 (not shown) or $40 \mu\text{M}$ (Figure 6), which indicates a first-order reaction, e.g., $\text{E}_1 \cdot \text{S}_{\text{off}} \rightarrow \text{E}_2 \cdot \text{S}_{\text{on}}$. The amplitudes and velocities were, however, dependent on the chosen binding protein. Thus, attachment of pB or fA to TC (Figure 6B) caused an almost immediate jump to the base-on form of the ligands. The following first-order phase was characterized by a low amplitude and a relatively high velocity [$k = 190 \text{ s}^{-1}$ (pB) and 60 s^{-1} (fA) in Figure 6B]. In the cases of HC and IF, the distribution of phases was completely opposite. Thus, both proteins attached the base-off ligands without a particular change in their constitution (small jumps in absorbance, Figure 6A,C). The following base-off \rightarrow base-on conversion was, however, characterized by large amplitudes and low rate constants [$k = 0.08 \text{ s}^{-1}$ for HC·fA (Figure 6A), and $k = 22 \text{ s}^{-1}$ for IF·fA and 20 s^{-1} for IF·pB (Figure 6C)].

Association of IF Fragments in the Presence of Cbl and Analogues. Two IF domains of 30 and 20 kDa (N-IF₃₀ peptide and IF₂₀-C glycopeptide, respectively; see ref 18 for details) were isolated as separated units and examined for their ability to associate in the presence of a ligand. Efficient assembly of the fragments into a stable IF₃₀·Cbl·IF₂₀ complex was demonstrated for CNCbl and H₂OCbl (9, 18). In this assay, a mixture of the peptides IF₃₀ and IF₂₀ (1.2:1) was exposed to a 2-fold excess of the ligand (AdoCbl, CBC, pB, or fA), whereupon the reactants were subjected to HPLC (Figure 7). The light scattering, refractive index, and ligand absorbance were recorded for the slices in the elution profiles.

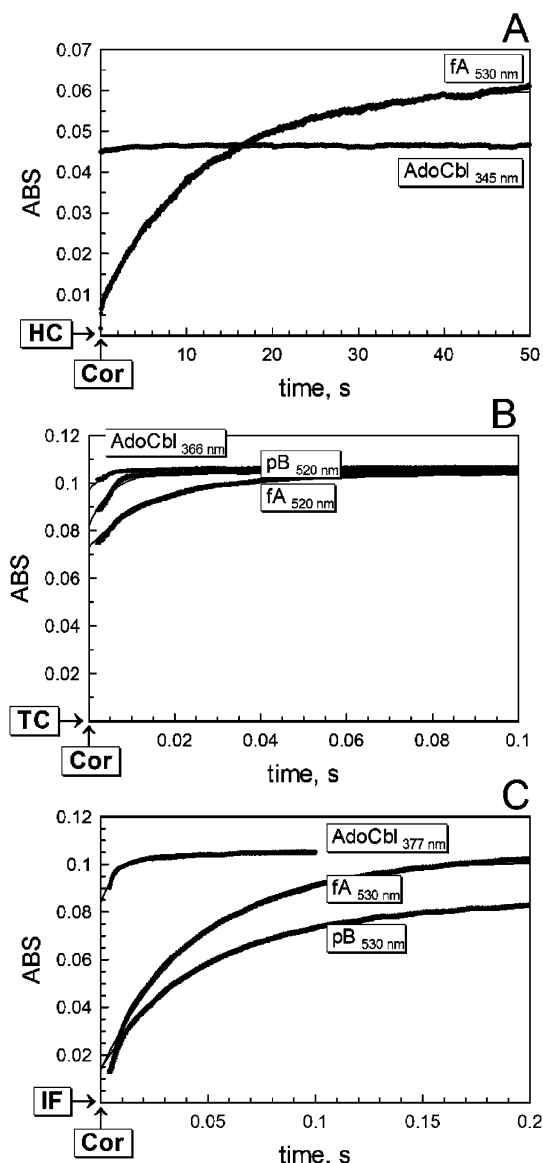


FIGURE 6: Kinetics of the base-off \rightarrow base-on transition induced by binding to the transporting proteins. Specific proteins (20 μ M) were mixed with ligands AdoCbl, pB, and fA (40 μ M) at pH 7.5 and 20 $^{\circ}$ C, and the transition in their absorbance was measured over time at the indicated wavelength. Transitions were induced by HC (A), TC (B), and IF (C).

The molar masses of the eluted components were calculated as described previously (18).

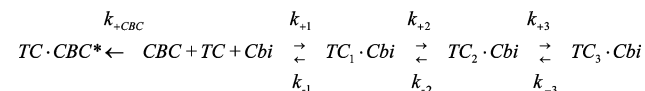
Both AdoCbl and the fluorescent analogue CBC assembled two fragments into a complex of 46 ± 1 kDa (Figure 7A,B). Base-off analogues did not initiate the protein association despite visible binding to the high-affinity fragment IF₂₀, as judged from the elevated ligand absorbance A_{340} (dashed-dotted line) in the IF₂₀ fractions (Figure 7C). A slightly increased A_{340} in the IF₃₀ fraction (Figure 7C) was probably caused by the optical density of the protein moiety IF₃₀ overlapped with IF \cdot pB absorbance. No essential attachment of pB to IF₃₀ was found in the individual binding experiment presented in Figure 7D. In the presence of pB or fA, the IF peptides were eluted as the two peaks of 27 ± 1 and 18 ± 1 kDa (the example for pB is shown in Figure 7C). Neither essential binding nor protein association was detected for Cbi and IF fragments under identical conditions (not shown).

Molecular features of IF₃₀ and IF₂₀ were also examined for each peptide separately (Figure 7D), and no change in their molecular masses was detected when different ligands were added. At the same time, significant saturation of the isolated fragment IF₂₀ (≈ 2 μ M in the peak) with AdoCbl ($\approx 90\%$) and pB ($\approx 40\%$) is visible on the gel filtration profiles (Figure 7D) according to the ligand absorbance at 340 nm (dashed-dotted lines). Saturation of IF₂₀ with CBC and Cbi under identical conditions corresponded to 90 and $<5\%$, respectively (not shown). Another fragment, IF₃₀, exhibited only marginal binding ability [see examples for AdoCbl and pB [Figure 7D (dashed-dotted lines)]]. The slightly elevated A_{340} in IF₃₀ fractions originated mainly from the residual absorbance of the protein peak at 280 nm.

General Fitting Models. Multiphasic character of the binding and dissociation was observed in many experiments and suggests that the ligand may form several complexes with a protein. These complexes are formed either concurrently (e.g., set of reactions $E_1 + S \leftrightarrow E_1S$, $E_2 + S \leftrightarrow E_2S$, ...) or sequentially, as a chain of conformational equilibria (e.g., $E_1 + S \leftrightarrow E_1S \leftrightarrow E_2S \leftrightarrow \dots$). Choosing between the first or second type of the model determines the approach to calculation of the equilibrium dissociation constant K_d . As each ligand demonstrated individual a distribution of phases (e.g., Table 2), the second scheme with multiple structural transitions seemed to be more probable. In the following section, the designed fitting models are discussed.

Modeling TC-Cbi Interactions. The full kinetic scheme was reconstructed in steps using the binding-dissociation experiments performed on different time scales and with different mixing orders. The successive analysis of the records in Figures 2B, 3B, and 4B allowed us to increase the complexity of the scheme step by step and estimate the values of k_{+1} , k_{-1} , k_{+2} , k_{-2} , k_{+3} , and k_{-3} , respectively. Additionally, the exponential fit in Figure 4B closely indicated the values of k_{-2} and k_{-3} . After preliminary evaluation, the rate constants were adjusted to satisfy the global fit of all the data. The calculations were performed with help of Gepasi 3 (22). The resulting model is depicted in Scheme 1

Scheme 1



where the rate constants ($k_{+CBC} = 68$, $k_{+1} = 17$, $k_{-1} = 0.7$, $k_{+2} = 0.4$, $k_{-2} = 0.2$, $k_{+3} = 0.013$, and $k_{-3} = 0.005$) are expressed in μ M⁻¹ s⁻¹ or s⁻¹. The monitored intermediate was TC \cdot CBC, and the assigned coefficient of fluorescence change (ΔF) was 0.82 RU/ μ M.

In the binding experiment [Figures 2B and 3B (dashed-dotted lines)], the following initial concentrations of the reactants were used: 0.5 μ M TC, 0.55 μ M CBC, and 0.55 μ M Cbi. In the dissociation experiment (Figure 4B), the simulations were divided into two steps. First, the transient concentrations of the intermediates were calculated for the mixture of 0.5 μ M TC and 0.55 μ M Cbi, with an incubation time 600 s. Second, 0.55 μ M CBC was introduced into the model, and time-dependent formation of TC \cdot CBC was simulated [Figure 4B (dashed-dotted line)].

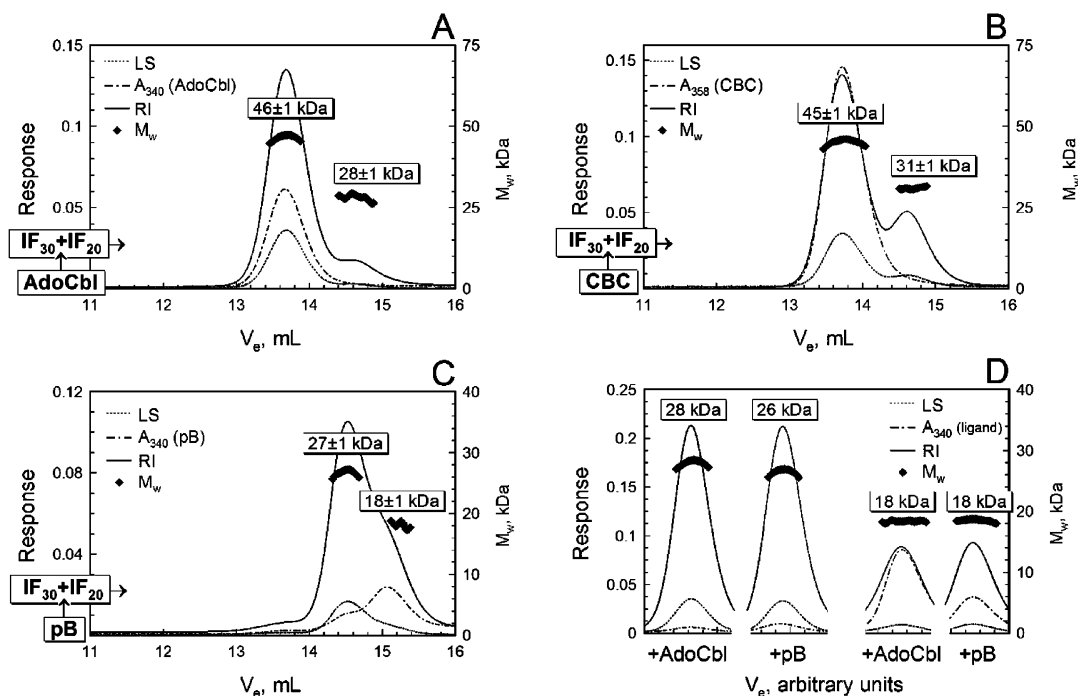


FIGURE 7: Association of IF fragments in the presence of Cbl and analogues. Two split fragments, IF₂₀ and IF₃₀, were incubated with different ligands and subjected to HPLC. The light scattering (LS), refractive index (RI), and absorbance (e.g., A₃₄₀) were measured in all fractions of the elution profiles. LS/RI ratios were used for calculation of the molecular masses of the peptides or their ligand complexes. Absorbance records revealed the presence of the bound ligand. Elution profiles of (A) the IF₂₀/IF₃₀/AdoCbl mixture (16, 17, and 30 μM, respectively), (B) the IF₂₀/IF₃₀/CBC mixture (16, 20, and 40 μM, respectively), (C) the IF₂₀/IF₃₀/pB mixture (16, 17, and 30 μM, respectively), and (D) individual peptides IF₃₀ with Cbl/pB (30 and 60 μM, respectively) and IF₂₀ with Cbl/pB (33 and 60 μM, respectively).

Table 2: Dissociation Rate Constants for Different Corrinoids at 20 °C and pH 7.5

	k_{-app} (s ⁻¹)		
	HC	TC	IF
CNCbl ^a	nd ^c	3×10^{-7}	4×10^{-7}
AdoCbl	$\approx 5 \times 10^{-7}$	$\approx 5 \times 10^{-7}$	$\approx 5 \times 10^{-7}$
CBC ^a	nd ^c	4×10^{-7}	24%, ^b 2×10^{-4} 62%, ^b 8×10^{-6}
pB/fA	$\approx 5 \times 10^{-7}$	6×10^{-6}	22%, ^b 3.5 24%, ^b 0.11 46%, ^b 0.012
Cbi	$\approx 5 \times 10^{-7}$	30%, ^b 0.2 55%, ^b 0.008	52%, ^b 4.5 22%, ^b 0.15 26%, ^b 0.017

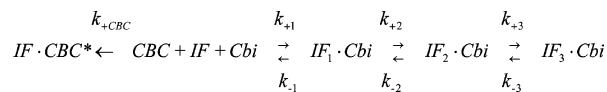
^a Data from ref 10. ^b Indicated values in percent correspond to the relative amplitudes of the phases of dissociation when fitting the dissociation curve by a multiexponential function. The corresponding rate coefficients immediately follow. ^c Not determined.

The scheme is in reasonable agreement with earlier kinetic data (11) on competition between Cbl and Cbi for the immobilized preparation of bovine TC (bovTC). Two forms of bovTC·Cbi were produced with approximate K_d values of 100 (15%) and 1 nM (85%). The above partition may correspond to the TC₁·Cbi and TC₃·Cbi complexes from this study (Scheme 1). In addition, a biphasic curve for dissociation of bovTC·Cbi (Figure 3B of ref 11) does resemble the current data in Figure 4B; however, all rate constants of the immobilized bovine protein (11) seem to be decreased by a factor of 10.

Modeling IF–Cbi Interactions. Reconstruction of the binding model for IF and Cbi was based on the principles analogous to those described in the above modeling example.

The rate constants ($k_{+CBC} = 77$, $k_{+1} = 57$, $k_{-1} = 9$, $k_{+2} = 1.0$, $k_{-2} = 0.6$, $k_{+3} = 0.02$, $k_{-3} = 0.02$) in Scheme 2

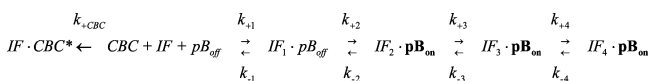
Scheme 2



are expressed in $\mu\text{M}^{-1} \text{s}^{-1}$ or s^{-1} , and ΔF for IF·CBC was 2.4 RU/μM. The simulations based on the calculated parameters are shown in Figures 2C, 3C, and 4C as dashed lines.

Modeling IF–pB and IF–fA Interactions. Binding of two base-off analogues, pB and fA, to IF required the most complex analysis, with the coordinative base-off → base-on transition included (Figure 6C). Our initial fitting model was based on the linear mechanism (Scheme 3)

Scheme 3



which was in agreement with the binding experiments in Figures 2C and 3C (long dashes). The fitting parameters were as follows: $k_{+CBC} = 77$, $k_{+1} = 70$, $k_{-1} = 7$, $k_{+2} = 20$, $k_{-2} = 3$, $k_{+3} = 0.2$, $k_{-3} = 0.1$, $k_{+4} = 0.02$, and $k_{-4} = 0.01$ expressed in $\mu\text{M}^{-1} \text{s}^{-1}$ or s^{-1} . $\Delta F = 2.4 \text{ RU}/\mu\text{M}$ for IF·CBC.

However, the dissociation experiment could not be fitted using the same scheme [Figure 4C (dotted line)]. None of the attempted adjustments in the rate constants helped to fit both binding and dissociation data equally well. Finally, the

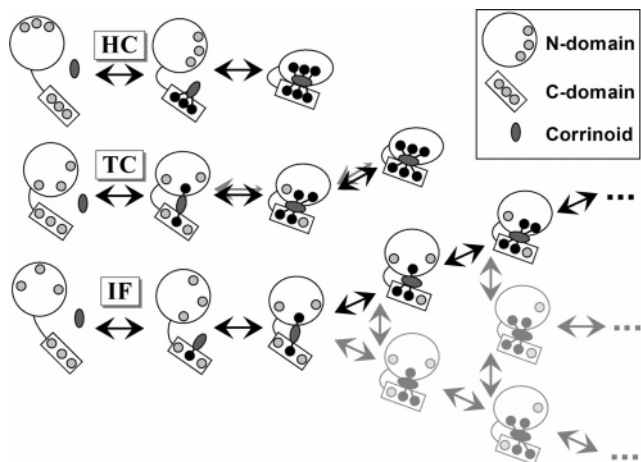


FIGURE 8: Models of binding of ligand to the specific transporting proteins. For HC, domains of apo-HC are spatially separated. Binding of ligands to HC is characterized by a minimal number of steps. For TC, domains of apo-TC act cooperatively and favor Cbl (Ado, CN, H₂O, ...) at the first encounter. Binding of ligands to TC includes several steps. For IF, domains of apo-IF are spatially separated, and ligand binding requires the maximal number of transitions. Alternative (and erroneous) routes of binding are suggested for the analogues (gray arrows).

Primary Protein–Ligand Contacts. The initial attachment of the corrinoids to the transporting proteins was examined in Figure 2, and the calculated rate constants (k_{+1}) are listed in Table 1. Most ligands were characterized by a k_{+1} of $6\text{--}8 \times 10^7 \text{ M}^{-1} \text{ s}^{-1}$. These values can be compared to the rate constant for encounters between a spheric ligand of Cbl size [radius $R_{\text{Cbl}} \approx 0.7 \text{ nm}$ (19); diffusion coefficient $D_{\text{Cbl}} \approx 5 \times 10^{-6} \text{ cm}^2/\text{s}$] and a shallow cavity (a disklike patch) of the binding site ($R_A \approx 2 \text{ nm} = 2 \times 10^7 \text{ cm}$) in the molecule of a 46 kDa protein with an $R_p \approx 3 \text{ nm}$ (19) and a $D_p \approx 7 \times 10^{-7} \text{ cm}^2/\text{s}$ using the appropriate equation (23, 24):

$$k_{+\text{coll}} = \frac{1}{2} \times 4 \times \frac{6 \times 10^{23}}{1000} (D_{\text{Cbl}} + D_p) R_A \left(1 + \frac{\pi R_{\text{Cbl}}}{2 R_A} \right) = 2 \times 10^9 \text{ M}^{-1} \text{ s}^{-1}$$

Other models predict even higher values of $k_{+\text{coll}}$ ($\approx 1 \times 10^{10} \text{ M}^{-1} \text{ s}^{-1}$) if the unspecific van der Waals forces, stabilizing a ligand at the surface of a protein, are taken into account (25). According to the estimated $k_{+1}/k_{+\text{coll}}$ ratio of ≤ 0.03 , one efficient encounter between Cbl and the specific binding site occurs in the course of 30 or more unproductive collisions. The calculations indicate that geometric requirements (key–lock?) for the efficient entry of a corrinoid into the binding pocket are possible, and the Cbl-specific proteins can potentially discriminate between different ligands already at the first contact. However, HC and IF bound all the ligands equally fast. This behavior is unexpected since the affinity of IF for Cbl analogues (pB, fA, and Cbi) is $10^6\text{--}10^7$ -fold lower than for the true substrate Cbl (Table 3). A severe decrease in the affinity points to essential incompatibility between Cbl analogues and the binding site of IF, yet the analogues attached to IF as fast as Cbl ($k_{+\text{analogue}} = k_{+\text{Cbl}}$); this effect deserves an explanation as it is contradictory to the key–lock model.

Similar k_{+1} values (Table 1) require comparable sizes and compositions of all colliding species which is obviously not the case (Figure 1). We can circumvent this contradiction

assuming that only the invariant parts of ligands (e.g., amide side chains) are involved in primary contacts with HC and IF. The primary binding site in these proteins can be allocated to the small C-terminal domain for the following reasons. (1) The C-terminal fragment IF₂₀ has a high affinity for ligands (see Figure 7D and refs 9, 10, and 18). (2) The rate of binding of Cbl and CBC to IF₂₀ ($k_{+1,\text{IF}20} = 60 \mu\text{M}^{-1} \text{ s}^{-1}$) resembles that for the full-length IF (Table 1) in contrast to IF₃₀ with a much lower binding rate constant $k_{+1,\text{IF}30}$ of $3 \mu\text{M}^{-1} \text{ s}^{-1}$ (10). The fact that attachment of convertible base-on ↔ base-off analogues pB and fA to the C-terminal fragment IF₂₀ was not accompanied by any significant change in the off–on balance supports the local character of this interactions. Reduction of the primary contact area ($R_{\text{Cbl}} = R_A \leq 0.4 \text{ nm}$) would decrease $k_{+\text{coll}}$ and increase the efficiency of encounters to 10% or more for all ligands. This value is sufficiently high to abandon the key–lock binding model and accept an unorganized architecture of the binding sites in the unsaturated IF and HC.

The mechanism of primary attachment of ligands to TC seems to be different from those of IF and HC. Thus, dispersion of k_{+1} for the binding of nonfluorescent corrinoids to TC was quite high (mean ± standard deviation = $100 \pm 45\%$). On the contrary, the same ligands bound to HC and IF with low dispersion in k_{+1} (100 ± 8 and $100 \pm 12\%$, respectively) (see Table 1). Variation in k_{+1} for TC does not look random since the rate constant decreased in parallel with the structural distortions of analogues (Table 1). The interaction of this protein with the ligands has slightly better agreement with the key–lock binding model, where an efficient encounter between a distorted analogue and the binding site is hampered. We can therefore assume that versatile protein–ligand contacts are established already at the initial step, possibly because both TC domains participate in inspection of the ligand from the opposite sides.

The suggested model of primary protein–ligand contacts is schematically depicted in Figure 8; see the first steps of the presented schemes.

Base-Off → Base-On Transition and Assembly of the Domains. Convertible base-off ↔ base-on analogues pB and fA (Figure 1) were particularly useful for examination of the protein-induced transitions within ligands, due to a pronounced shift in their absorbance spectra following any change in the off–on balance (Figure 5). This spectral pattern was recently studied with an anti-B₁₂ antibody raised against AdoCbl. Analysis by UV–vis absorbance spectroscopy indicated that the antibody bound all three adenosyl cobamides (AdoCbl, as well as pB and fA) in their base-on forms (26).

Here we found that binding of pB and fA to any of the assayed proteins caused a base-off → base-on transition, although rates and apparent amplitudes varied (Figure 6). Again, unexpected similarity in the features of HC and IF was found. Thus, the initial attachment of these ligands to HC and IF caused no significant change in the off–on balance (Figure 6A,C), confirming the local character of primary contacts. Then, a slow and incomplete transformation from the base-off to base-on form was observed spectroscopically (compare panels A and C of Figures 5 and 6). Incomplete transitions can be interpreted as either uniform locking of all ligand molecules in some intermediate coordination structure or their distribution between two

directly opposite structures (base-off and base-on). The data for HC did not allow any reliable prognosis. However, analysis of IF kinetics according to the latter model (e.g., Scheme 4) pointed to the following balance between the ligand forms, $IF_1 \cdot pB_{\text{off}}$ (20%) and $IF_2 \cdot pB_{\text{on}}$ (80%), which seem to be distributed between numerous protein–ligand conformations (see Figure 8, bottom sketch).

Interaction of pB and fA with TC dramatically differed from interaction of HC and IF. Thus, a very fast and efficient base-off \rightarrow base-on transformation was observed upon binding to TC, and 70–80% of the reaction was accomplished during the primary attachment (Figure 6B). In other words, the first contacts between TC and a base-off corrinoid induced a major rearrangement of the ligand. Complete coordination of the base followed close in time, and pB and fA were uniformly trapped by TC in the base-on form.

We associate the observed transition of the base-off corrinoids pB and fA to their base-on form with the assembly of the protein domains, directly shown for the IF fragments upon interaction with Cbl or CBC (see Figure 7A,B and refs 10 and 18). The assembly is followed by an induced fit of the ligand. This conjecture is in agreement with the crystallographic data for TC (19), where the protein residues from both N- and C-binding units are in contact with the nucleotide loop of Cbl. These links can easily fit a loosely organized base-off ligand to the correct shape, compatible with the binding site. However, this transformation occurs with a different velocity and efficiency depending on the protein used. We can explain the difference between TC, on the one hand, and HC and IF on the other by simultaneous and sequential action of the protein domains, respectively. For instance, the mutual orientation and simultaneous action of the two TC domains favor from the very beginning a Cbl-resembling structure. On the other hand, domains of apo-HC and apo-IF seem to be spatially separated. A ligand binds to the latter proteins in two major steps: (i) attachment to the C-terminal segment and (ii) assembly of the C- and N-terminal segments into a joined complex with the ligand between them. Accommodation of ligands is always efficient in HC (Table 3) in contrast to IF, where interplay between the domains is ruined by an improper structure of ligand. An inability to form a triple protein–ligand–protein complex was directly demonstrated in the chromatographic experiments with the mixtures of IF fragments IF_{30} and IF_{20} (counterparts of N- and C-domains) and base-off and baseless analogues (Figure 7C). We hypothesize that correct positioning of the nucleotide plays a crucial role in the domain–domain association. This conjecture is supported by earlier observation, where a supplement of the separate nucleotide ribazole moiety improved the binding of baseless analogue Cbi to IF (5).

Final Stabilization of the Protein–Ligand Complex. We have only limited information about fixation of the ligands on HC because all corrinoids were attached to this carrier almost instantly with sufficiently high strength (Figure 2A). The data simulations according to Scheme 7 and Figure 8 (upper sketch) provide an uncontroversial two-step binding mechanism for a base-off ligand: (i) firm attachment to the C-terminal segment with a K_d of ≤ 10 pM and (ii) assembly of N- and C-terminal domains with or without an essential improvement in affinity (depending on the balance between

the rate constants). A similar binding pattern, although with varying rate constants, can be anticipated for other ligands. All in all, the binding kinetics of the least specific protein HC was characterized by a minimal number of detected steps. Accordingly, the process of ligand binding goes via multiple protein–ligand contacts (see the schematic presentation in the top line of Figure 8). The involvement of numerous bonds at each elementary binding stage would overcome inconsistency in the ligand structure by sheer force and fit a corrinoid into the binding site of HC.

More information about ligand fixation was drawn from the TC kinetics. As previously discussed, the primary binding step probably involved almost simultaneous attachment of a ligand to the two protein macro blocks (Figure 8, middle line). The K_d value at this step can be evaluated as being < 50 nM even for Cbi. Then, gradual adjustments on the subdomain level seemed to take place, and they were accompanied by improved fixation of the bound ligand. Analysis of the binding–dissociation curves for the baseless corrinoid Cbi indicated the presence of at least two stabilization steps, which followed the primary attachment of this analogue (Figures 3B and 4B and Scheme 1). Finally, Cbi was distributed among three TC·Cbi complexes with different dissociation stabilities (Scheme 1), and their overall equilibrium dissociation constant corresponded to 5 nM (Table 3). The other ligands are expected to follow a similar binding route, where a better resemblance to Cbl favors faster formation of the final firm complex.

The highest complexity of kinetics was detected for the most Cbl-specific protein IF. Here we observe numerous stabilization steps for all analogues, while the apparent K_d decreases from 100–200 to 5–50 nM. Finally, each analogue becomes distributed among several IF complexes of varying stability (Tables 2 and 3 and Schemes 2 and 4). The route of binding seems to be predetermined by the initial structure of each particular corrinoid. While the true substrate Cbl proceeds to the final firm complex $IF_n \cdot Cbl$, an analogue slowly follows deviating and unaccomplished routes (Figure 8, bottom sketch, black and gray arrows, respectively).

Unexpectedly, the ligands with modifications in the nucleotide loop (CBC, pB, and fA) were prone to branched binding routes when interacting with IF (Schemes 4 and 5). It seems that the N- and C-domains of IF can interact in alternative ways depending on the conditions of their initial collision. The adverse effect of the nucleotide substitution upon assembly of split domains was directly demonstrated for the mixtures of IF fragments with pB (Figure 7C), fA, or Cbi (not shown). An essentially disperse organization of the unsaturated protein and the requirement of a strict order in protein–ligand interactions seem to be responsible for such behavior of IF. We can speculate whether the multistep kinetics is a general prerequisite of highly specific ligand binding. Thus, interruption of the binding sequence and/or gradual accumulation of structural errors in the binding site is more probable in this case.

It should be mentioned that the relative affinities for analogues ($K_{\text{analogue}}/K_{\text{Cbl}}$) measured by the isotope dilution method (Determination of Relative Affinities) reproducibly deviated from the values obtained by kinetic studies (Table 3). Thus, the difference between an analogue and Cbl seems to be underestimated during the isotope dilution assay, at

least for TC and IF. The possible kinetic background of this effect was discussed previously (11).

Physiological Implication. We have found that the binding of different Cbl analogues to TC and IF obeys a complex kinetics. If these effects are not taken into account, measurement of affinity may result in an essential error. Our approach allowed to calculate the K_d^{app} of the overall equilibrium $E + S \leftrightarrow \sum(E_iS)$ in concentration units (Table 3) and estimate whether it is possible to saturate the specific proteins with structurally deviating corrinoids under physiological conditions. According to a general belief, weak binding of analogues precludes saturation of IF and TC with antimetabolites of Cbl. The current data, however, show that even a baseless corrinoid Cbi can bind to IF and TC with K_d^{app} values of 40 and 5 nM, respectively (Table 3). This is sufficient to partially saturate intestinal IF (10–100 nM) or plasma TC (0.2–1 nM) and mediate transportation of “wrong” corrinoids. Preliminary results on the binding of IF–analogue complexes to the specific intestinal receptor cubilin point to their interaction, as soon as IF becomes sufficiently saturated with any Cbl-resembling ligand (unpublished). A more detailed account will be presented in a separate publication. In this regard, possible proteolytic splitting of unsaturated apo-IF into two fragments can be physiologically significant, since several natural analogues were incapable of assembling IF₃₀ and IF₂₀ into a stable complex (Figure 7C) with a high affinity for the receptor (9).

The physiological role of the third Cbl-transporting protein, HC (R-binder), should also be discussed. This unspecific binder is present in many body fluids (e.g., saliva, stomach juice, and plasma); however, its function remains obscure. The performed kinetic analysis demonstrates that HC can efficiently sequester many analogues (e.g., pB and Cbi) which would otherwise be bound to IF and TC. Calculations show that intestinal IF (50 nM) will be depleted of Cbi and pB (5 nM) in 100–200 s if 10 nM HC is present. Despite splitting into two to three segments (27), HC partially retains its Cbl binding capacity after several hours in the intestinal juice (27, 28), and its active fragments were found even in feces (29). This is a strong indication that HC can be associated with clearance of dietary Cbl analogues. The relative stability of many TC–analogue complexes may hinder fulfillment of the same task in plasma, yet Cbi would be definitely transferred to HC. The protective role of HC remains generally unexplored, though some measurements point to the presence of inactive Cbl derivatives in blood and tissues (30, 31).

The presented experimental results have another implication: they are of importance for synthesis and application of new Cbl conjugates with imaging or therapeutic properties (13, 14). Calculations evidently demonstrate that even a 1000-fold decrease in affinity (e.g., $K_d^{\text{app}} \approx 5$ pM, $k_+ \approx 50 \times 10^6 \text{ M}^{-1} \text{ s}^{-1}$, $k_- \approx 2.5 \times 10^{-4} \text{ s}^{-1}$) would not prevent an analogue from being bound to IF and TC under physiological conditions. This estimation essentially broadens the choice of conjugation techniques.

Conclusions. In this publication, we for the first time present the values of the dissociation constants, expressed in concentration units, for several Cbl analogues and Cbl-transporting proteins. It appeared that the binding followed a multistep mechanism, which was particularly evident for

the most specific protein IF. The binding step, crucial for specific recognition of ligands by IF and TC, can be attributed to mutual rearrangements of the protein domains after being assembled by ligand into a preliminary complex. Correct assembly is, therefore, critically important for strong retention of a ligand. These investigations strongly suggest that saturation of IF and TC with analogues is essentially alleviated under physiological conditions by the presence of HC.

REFERENCES

- Kräutler, B., and Ostermann, S. (2003) Structure, reactions, and functions of B₁₂ and B₁₂-proteins, in *The porphyrin handbook* (Kadish, K. M., Smith, K. M., and Guilard, R., Eds.) Vol. 11, pp 229–276, Elsevier Science, New York.
- Nexø, E. (1998) Cobalamin binding proteins, in *Vitamin B₁₂ and B₁₂-Proteins* (Kräutler, B., Arigoni, D., and Golding, T., Eds.) pp 461–475, Wiley-VCH, Weinheim, Germany.
- Moestrup, S. K., and Verroust, P. J. (2001) Megalin- and cubilin-mediated endocytosis of protein-bound vitamins, lipids, and hormones in polarized epithelia, *Annu. Rev. Nutr.* 21, 407–428.
- Kolhouse, J. F., and Allen, R. H. (1977) Absorption, plasma transport, and cellular retention of cobalamin analogues in the rabbit. Evidence, for the existence of multiple mechanisms that prevent the absorption, and tissue dissemination of naturally occurring cobalamin analogues, *J. Clin. Invest.* 60, 1381–1392.
- Andrews, E. R., Pratt, J. M., and Brown, K. L. (1991) Molecular recognition in the binding of vitamin B₁₂ by the cobalamin-specific intrinsic factor, *FEBS Lett.* 281, 90–92.
- Marchaj, A., Jacobsen, D. W., Savon, S. R., and Brown, K. L. (1995) Kinetics and thermodynamics of the interaction of cyanocobalamin (vitamin B₁₂) with haptocorrin: Measurement of the highest protein-ligand binding constant yet reported, *J. Am. Chem. Soc.* 117, 11640–11646.
- Fedosov, S. N., Berglund, L., Fedosova, N. U., Nexø, E., and Petersen, T. E. (2002) Comparative analysis of cobalamin binding kinetics and ligand protection for intrinsic factor, transcobalamin, and haptocorrin, *J. Biol. Chem.* 274, 26015–26020.
- Cannon, M. J., Myszk, D. G., Bagnato, J. D., Alpers, D. H., West, F. G., and Grissom, C. B. (2002) Equilibrium and kinetic analysis of the interactions between vitamin B(12) binding proteins and cobalamins by surface plasmon resonance, *Anal. Biochem.* 305, 1–9.
- Fedosov, S. N., Fedosova, N. U., Berglund, L., Moestrup, S. K., Nexø, E., and Petersen, T. E. (2005) Composite organization of the cobalamin binding and cubilin recognition sites of intrinsic factor, *Biochemistry* 44, 3604–3614.
- Fedosov, S. N., Grissom, C. B., Fedosova, N. U., Moestrup, S. K., Nexø, E., and Petersen, T. E. (2006) Application of a fluorescent Cbl analogue for analysis of the binding kinetics. A study employing recombinant human transcobalamin and intrinsic factor, *FEBS Lett.* 273, 4742–4753.
- Fedosov, S. N., Petersen, T. E., and Nexø, E. (1995) Binding of cobalamin and cobinamide to transcobalamin from bovine milk, *Biochemistry* 34, 16082–16087.
- Stupperich, E., and Nexø, E. (1991) Effect of the cobalt-N coordination on the cobamide recognition by the human vitamin B₁₂ binding proteins intrinsic factor, transcobalamin and haptocorrin, *Eur. J. Biochem.* 199, 299–303.
- Russell-Jones, G. J. (1998) Use of vitamin B₁₂ conjugates to deliver protein drugs by the oral route, *Crit. Rev. Ther. Drug Carrier Syst.* 15, 557–586.
- Collins, D. A., Hogenkamp, H. P., O'Connor, M. K., Naylor, S., Benson, L. M., Hardyman, T. J., and Thorson, L. M. (2000) Biodistribution of radiolabeled adenosylcobalamin in patients diagnosed with various malignancies, *Mayo Clin. Proc.* 75, 568–580.
- Fedosov, S. N., Berglund, L., Nexø, E., and Petersen, T. E. (1999) Sequence, S-S bridges, and spectra of bovine transcobalamin expressed in *Pichia pastoris*, *J. Biol. Chem.* 274, 26015–26020.
- Fedosov, S. N., Fedosova, N. U., Nexø, E., and Petersen, T. E. (2000) Conformational changes of transcobalamin induced by aquocobalamin binding. Mechanism of substitution of the cobalt-coordinated group in the bound ligand, *J. Biol. Chem.* 275, 11791–11798.

17. Fedosov, S. N., Laursen, N. B., Nexø, E., Moestrup, S. K., Petersen, T. E., Erik, Ø. Jensen, E. Ø., and Berglund, L. (2003) Human intrinsic factor expressed in the plant *Arabidopsis thaliana*, *Eur. J. Biochem.* 270, 3362–3367.
18. Fedosov, S. N., Fedosova, N. U., Berglund, L., Moestrup, S. K., Nexø, E., and Petersen, T. E. (2004) Assembly of the intrinsic factor domains and oligomerization of the protein in the presence of cobalamin, *Biochemistry* 43, 15095–15102.
19. Wuerges, J., Garau, G., Geremia, S., Fedosov, S. N., Petersen, T. E., and Randaccio, L. (2006) Structural basis for mammalian vitamin B₁₂ transport by transcobalamin, *Proc. Natl. Acad. Sci. U.S.A.* 103, 4386–4391.
20. Fieber, W., Hoffmann, B., Schmidt, W., Stupperich, E., Konrat, R., and Kräutler, B. (2002) Pseudocoenzyme B12 and adenosylfactor A: Electrochemical synthesis and spectroscopic analysis of two natural B12 coenzymes with predominantly base-off constitution, *Helv. Chim. Acta* 85, 927–944.
21. Nexø, E., Olesen, H., Norredam, K., and Schwartz, M. (1975) A rare case of megaloblastic anaemia caused by disturbances in the plasma cobalamin binding proteins in a patient with hepatocellular carcinoma, *Scand. J. Haematol.* 14, 320–327.
22. Mendes, P. (1997) Biochemistry by numbers: Simulation of biochemical pathways with Gepasi 3, *Trends Biochem. Sci.* 22, 361–363.
23. Eigen, M. (1974) Diffusion control in biochemical reactions, in *Quantum Statistical Mechanics in the Natural Science* (Kursunoglu, B., Mintz, S. L., and Widmayer, S. M., Eds.) pp 37–61, Plenum Publishing Co., New York.
24. van Holde, K. E. (2002) A hypothesis concerning diffusion-limited protein-ligand interactions, *Biophys. Chem.* 101–102, 249–254.
25. Zhou, G., Wong, M.-T., and Zhou, G.-Q. (1983) Diffusion-controlled reactions of enzymes. An approximate analytic solution of Chou's model, *Biophys. Chem.* 18, 125–132.
26. Hannak, R. B., Konrat, R., Schüller, W., Kräutler, B., Auditor, M.-T. M., and Hilvert, D. (2002) An antibody that reconstitutes the “base-on” form of B₁₂ coenzymes, *Angew. Chem., Int. Ed.* 41, 3613–3616.
27. Allen, R. H., Seetharam, B., Podell, E., and Alpers, D. H. (1978) Effect of proteolytic enzymes on the binding of cobalamin to R protein and intrinsic factor. In vitro evidence that a failure to partially degrade R protein is responsible for cobalamin malabsorption in pancreatic insufficiency, *J. Clin. Invest.* 61, 47–54.
28. Marcoullis, G., Nicolas, J. P., Parmentier, Y., Jimenez, M., and Gerard, P. (1980) A derivative of R-type cyanocobalamin binding proteins in the human intestine. A candidate antibacterial molecule, *Biochim. Biophys. Acta* 633, 289–294.
29. Gueant, J. L., Vidailhet, M., Pasquet, C., Djalali, M., and Nicolas, J. P. (1994) Effect of pancreatic extracts on the faecal excretion and on the serum concentration of cobalamin and cobalamin analogues in cystic fibrosis, *Clin. Chim. Acta* 137, 33–41.
30. Kolhouse, F., Kondo, H., Allen, N. C., Podell, E., and Allen, R. H. (1978) Cobalamin analogues are present in human plasma and can mask cobalamin deficiency because current radioisotope dilution assays are not specific for true cobalamin, *N. Engl. J. Med.* 299, 785–792.
31. Kondo, H., Kolhouse, F., and Allen, R. H. (1980) Presence of cobalamin analogues in animal tissues, *Proc. Natl. Acad. Sci. U.S.A.* 77, 817–821.

BI062063L